Supporting Information

Chemical and Mechanistic Analysis of Photodynamic Inhibition of Alzheimer's β-Amyloid Aggregation

Minkoo Ahn[1,†], Byung Il Lee[2,†], Sean Chia[1], Johnny Habchi[1], Janet R. Kumita[1], Michele Vendruscolo[1], Christopher M. Dobson[1,*] and Chan Beum Park[2,*]

[1] Centre for Misfolding Diseases, Department of Chemistry, University of Cambridge, Lensfield Road, Cambridge, CB2 1EW, UK. [2] KAIST Institute for the BioCentury, Department of Materials Science and Engineering, Korea Advanced Institute of Science and Technology (KAIST), Daejeon 305-701, Korea. [†] These authors contributed equally to this work. *Correspondence: Christopher M. Dobson (email: cmd44@cam.ac.uk), Chan Beum Park, (email: parkcb@kaist.ac.kr)

METHODS

Incubation of $A\beta_{42}$ with ThT under LED irradiation. For CD, NMR and kinetic experiments, aliquots of solution of $A\beta_{42}$ in glass vials were incubated for different times in the absence or presence of ThT at 4 or 30°C with LED irradiation. White LED light was used as the light source for all light conditions, except for the experiment where different light sources (red, blue and green LED) were used.

Circular dichroism (CD) spectroscopy. Recombinant β-amyloid (1-42) was purchased from rPeptide Co. (Watkinsville, GA). Monomeric $A\beta_{42}$ was prepared by dissolving the peptide in hexafluoro-2-propanol (HFIP) followed by sonication for 30 min and keeping it overnight at room temperature. Aliquots of the solution were put into 1.5 ml protein low-binding Eppendorf tubes and vacuum-dried for 2~3 h. The tubes were then stored at -20°C prior to the experiments when aliquots were dissolved in a buffer composed of CH_3CN (144 μM), Na_2CO_3 (144 μM) and NaOH (8.5 mM) and briefly sonicated for 1 min. The solutions were then diluted with phosphate buffer (8.5 mM) containing NaCl (8.5 mM), Na_2CO_3 (14 μM), NaOH (0.85 mM), and 6.0 % acetonitrile (final pH 8.0) to yield a final concentration of 40 μM of monomeric $A\beta_{42}$. To monitor the aggregation process, the solutions were incubated

in the absence or presence of ThT at 30°C for 24 h under dark or light conditions. After the incubation of 40 μM Aβ under various conditions at 30°C for 24 h, far-UV CD spectra were measured using a JASCO J-810 (Jasco Ltd, Great Dunmow, UK) spectropolarimeter at 20°C.

Atomic Force Microscopy (AFM). For the AFM measurements, 5 μl aliquots of the $A\beta_{42}$ sample solutions were deposited onto a cleaved mica substrate for 10 min and were rinsed several times with DI water to remove any remaining salts and unbound peptides. After the mica was fully dried, AFM images were acquired in tapping mode with an NCHR silicon cantilever (Nanosensors™, Neuchâtel, Switzerland) using a Multimode AFM instrument equipped with a Nanoscope III controller and "E"-type scanner (Bruker Nano Surfaces, Santa Barbara, CA).

Nuclear magnetic resonance (NMR) spectroscopy. For NMR experiments, ^{15}N-$A\beta_{42}$ was purified as previously described except that the buffer of the gel filtration step was changed to 50 mM ammonium acetate (pH 8.5).[1] Lyophilized ^{15}N-$A\beta_{42}$ was dissolved at an approximate concentration of 1 mM in 0.2% (vol/vol) ammonium solution and then collected and stored in aliquots at −80 °C until use. NMR samples were prepared by dissolving the lyophilized powder in 20 mM sodium phosphate buffer (pH 7.4) at a concentration of 20 μM containing 10 % (vol/vol) $^{2}H_2O$ in the presence and absence of equimolar concentrations of ThT in 1% DMSO. In order to understand the photodynamic effect of ThT on the structure of monomeric $A\beta_{42}$, not on the aggregated species, the monomeric samples were pre-incubated under dark or light conditions at 4 °C for each incubation time before NMR spectra were recorded. The NMR measurements were made on a Bruker AVANCE 700-MHz spectrometer equipped with a cryogenic probe (Bruker, Coventry, UK) with the probe temperature set to 278 K. ^{1}H-^{15}N heteronuclear single-quantum correlation (HSQC) spectra were recorded at a ^{1}H observation frequency of 700 MHz with 64 (t_1) × 1,024

(t_2) complex points and 32 scans per t_1 increment. The spectral width was 1,631 Hz for the ^{15}N dimension and 10,504 Hz for the ^{1}H dimension. Chemical shift perturbations (CSPs) and intensity changes were monitored using ^{1}H-^{15}N HSQC spectra. All NMR spectra were processed by NMRPipe,[2] and resonance assignment and intensity calculations were performed using the program Sparky (https://www.cgl.ucsf.edu/home/sparky/). The sample preparation protocol and the low NMR probe temperature (5 °C) were chosen to ensure that there is no aggregation of $A\beta_{42}$ during the entire data acquisition process. ^{15}N SORDID (signal optimization with recovery in diffusion delays) diffusion spectra were recorded with two gradient strengths (G = 10.4, 69.5% G_{max}) and a diffusion delay of Δ = 190 ms as previously discussed.[3]

Trypsin proteolysis LC-MS/MS. Gel bands were cut into 1mm^2 pieces, destained, reduced (DTT) and alkylated (iodoacetamide), and then subjected to enzymatic digestion with trypsin overnight at 37 °C. After digestion, the supernatants were pipetted into sample vials and loaded onto an autosampler for automated LC-MS/MS analysis. All LC-MS/MS experiments were performed using a nanoAcquity UPLC (Waters Corp., Milford, MA) system and an LTQ Orbitrap Velos hybrid ion trap mass spectrometer (Thermo Scientific, Waltham, MA). Separation of peptide fragments was performed by reverse-phase chromatography using a Waters reverse-phase nano column (BEH C18, 75 µm i.d. x 250 mm, 1.7 µm particle size) at a flow rate of 300 nL/min. The resulting samples were initially loaded onto a pre-column (Waters UPLC Trap Symmetry C18, 180 µm i.d x 20mm, 5 µm particle size) from the nanoAcquity sample manager with 0.1% formic acid for 5 min at a flow rate of 5 µL/min. After this time, the column valve was switched to allow the elution of peptides from the pre-column onto the analytical column. Solvent A was water + 0.1% formic acid and solvent B was acetonitrile + 0.1% formic acid. The linear gradient employed

was 5 - 40% B in 30 min, followed by a wash step and re-equilibration, and the total run time was 60 min.

The LC eluant was injected into the mass spectrometer by means of a nanospray source. All m/z values of eluting ions were measured in the Orbitrap Velos mass analyzer, set at a resolution of 30,000. Data dependent scans (Top 20) were employed to isolate and generate fragment ions automatically by collision-induced dissociation in the linear ion trap, resulting in MS/MS spectra. Ions with charge states of 2+ and above were selected for fragmentation. The resulting data were processed using Protein Discoverer (version 2.1., ThermoFisher, Waltham, MA). Briefly, all MS/MS data were converted to mgf files and the files were then submitted to the Mascot search algorithm (Matrix Science, London, UK) and searched against a customised database containing the target protein and common contaminant sequences (115 sequences, 38,274 residues; http://www.thegpm.org/crap/). Variable modifications of oxidation (M, H, W and Y), deamidation (NQ) and carbamidomethyl were applied. The peptide and fragment mass tolerances were set to 25ppm and 0.8 Da, respectively, and a significance threshold value of $p < 0.05$ and a peptide cut-off score of 20 were also applied.

Preparation of $A\beta_{42}$ for kinetic experiments. The kinetic experiments were carried out using recombinant $A\beta_{42}$ that was expressed and purified as described previously.[1] T monomeric $A\beta_{42}$ were prepared by dissolving the lyophilized $A\beta_{42}$ peptide in 6 M GdnHCl. The monomeric peptides were purified from potential oligomeric species and salt using a Superdex 75 10⁄300 GL column (GE Healthcare, Amersham, UK) on an AKTA Pure purification system (GE Healthcare) at a flow rate of 0.5 mL/min, and $A\beta_{42}$ was eluted in 20 mM sodium phosphate buffer, pH 8, supplemented with 200 μM EDTA and 0.02% NaN_3. The center of the peak was collected and the $A\beta_{42}$ concentration was determined from the absorbance of the

integrated peak area using ε_{280} = 1,490 $M^{-1} \cdot cm^{-1}$. The resulting $A\beta_{42}$ monomers were diluted with buffer to the desired concentration and incubated with different concentrations of ThT either under dark or light conditions. For the kinetics experiments in Fig. 2a, d, and e monomeric $A\beta_{42}$ was pre-incubated for 20 hr at 4 °C, as for the NMR and MS experiments, in order to understand the effects of photoexcited ThT on the aggregation propensity of the monomeric state of the peptide. Prior to the kinetic assays, the samples were supplemented with a further 20 μM of ThT from a 2 mM stock for the fluorescence measurements. All samples were prepared in low-binding Eppendorf tubes on ice using careful pipetting to avoid introduction of air bubbles. Each sample was then pipetted into multiple wells of a 96-well half-area, low-binding, clear- bottom, and PEG-coating plate (Corning; 3881), 80 μL per well.

Kinetic assays. Assays were initiated by placing the 96-well plate at 37 °C under quiescent conditions in a plate reader (Fluostar Omega, Fluostar Optima, or Fluostar Galaxy; BMGLabtech, Aylesbury, UK).[4] The ThT fluorescence was measured through the bottom of the plate with a 440 nm excitation filter and a 480 nm emission filter. The ThT fluorescence was followed for three repeats of each sample.

Theoretical analysis. The time evolution of the total fibril mass concentration, M(t), is described by the following integrated rate law.[5]

$$\frac{M(t)}{M(\infty)} = 1 - \left(\frac{B_+ + C_+ \quad B_- + C_+ e^{\kappa t}}{B_+ + C_+ e^{\kappa t} \quad B_- + C_+} \right)^{\frac{k_\infty^2}{\kappa \bar{k}_\infty}} e^{-k_\infty t}$$

To capture the complete assembly process, only two particular combinations of the rate constants define most of the macroscopic behavior, those related to the rate of formation of new aggregates through primary pathways $\lambda = \sqrt{2k_+ k_n m(0)^{n_c}}$ and through secondary pathways $\kappa = \sqrt{2k_+ k_2 m(0)^{n_2+1}}$, where the initial concentration of soluble

monomers is denoted by $m(0)$, n_c and n_2 describe the dependencies of the primary and secondary pathways on the monomer concentration, and k_n, k_+ and k_2 are the rate constants of primary nucleation, elongation and secondary nucleation, respectively.

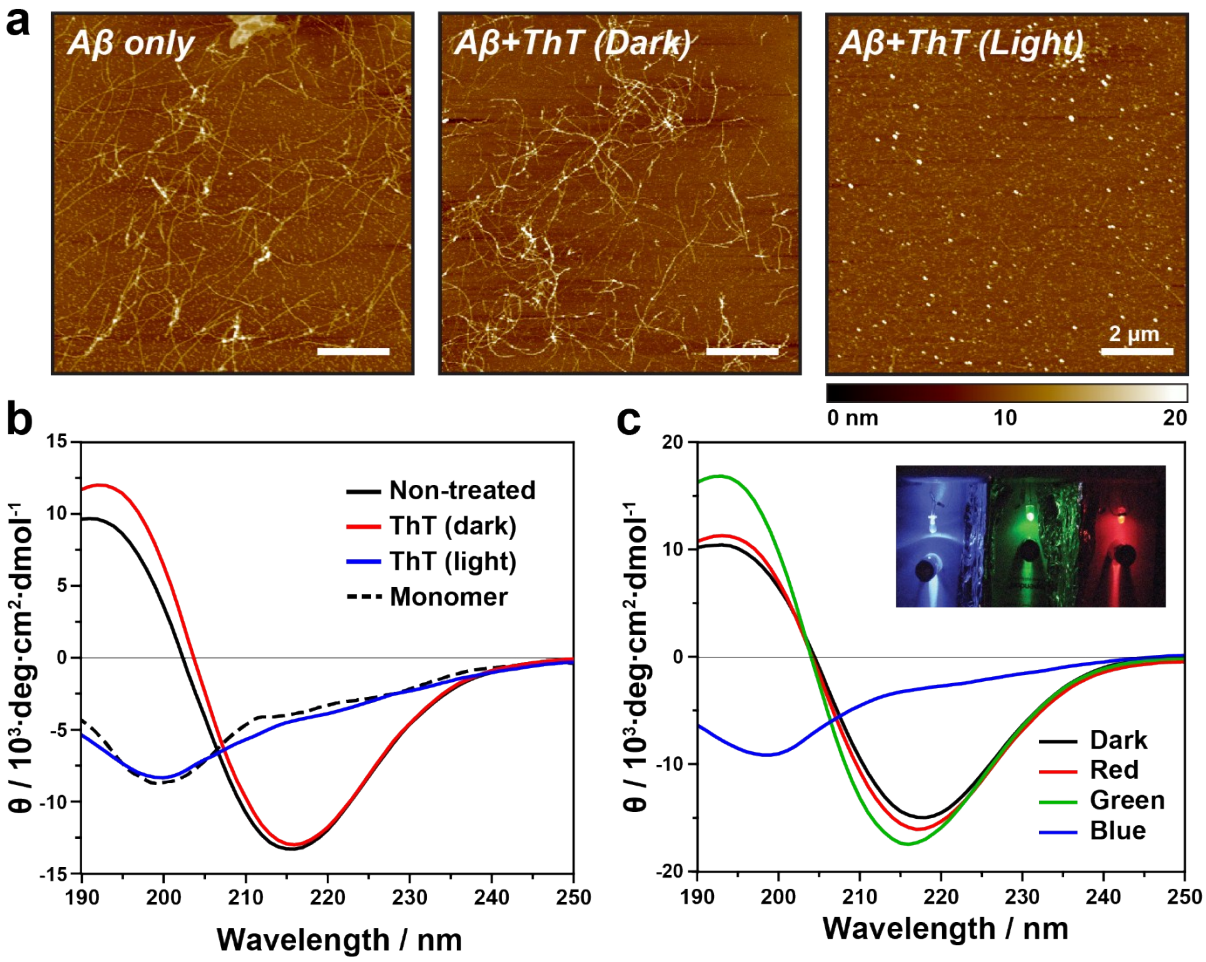

Figure S1. The inhibitory activity of photosensitized ThT on $A\beta_{42}$ aggregation monitored by AFM and CD. (a) AFM images and (b) CD spectra of $A\beta_{42}$ incubated in the presence of ThT (10 μM) under dark and light conditions at 30°C for 24 hr. No fibrils could be observed in the $A\beta_{42}$ sample treated with ThT in the presence of light. Scale bar: 2 μm. In the CD spectra, no detectable β-sheet structure was formed when $A\beta_{42}$ was treated with photo-excited ThT, implying that the $A\beta_{42}$ monomers did not self-assemble into aggregates. (c) Effect of wavelength of the incident light on the inhibitory activity of ThT. The red, blue and green LEDs utilized in this experiment are shown in inset.

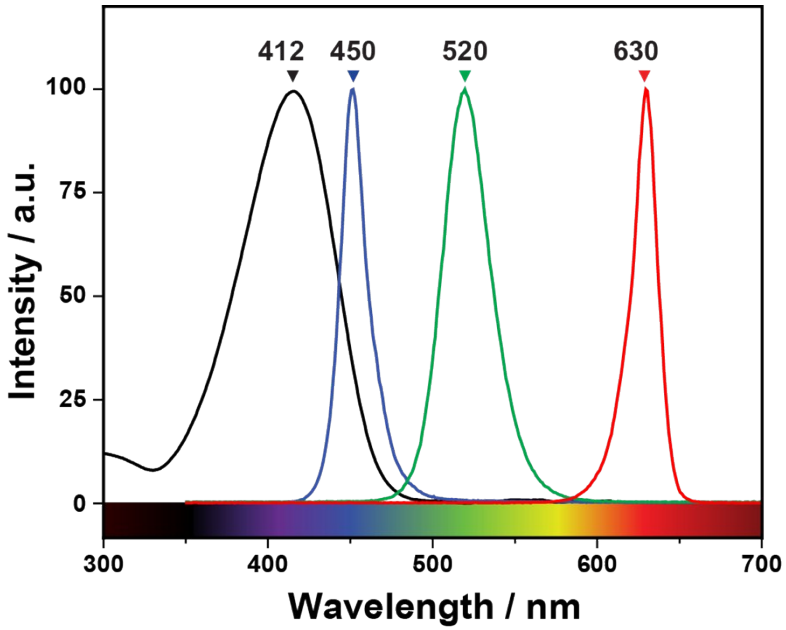

Figure S2. Absorbance spectrum of ThT (black line) and the emission spectra of the three colored LEDs that were utilized in the experiments.

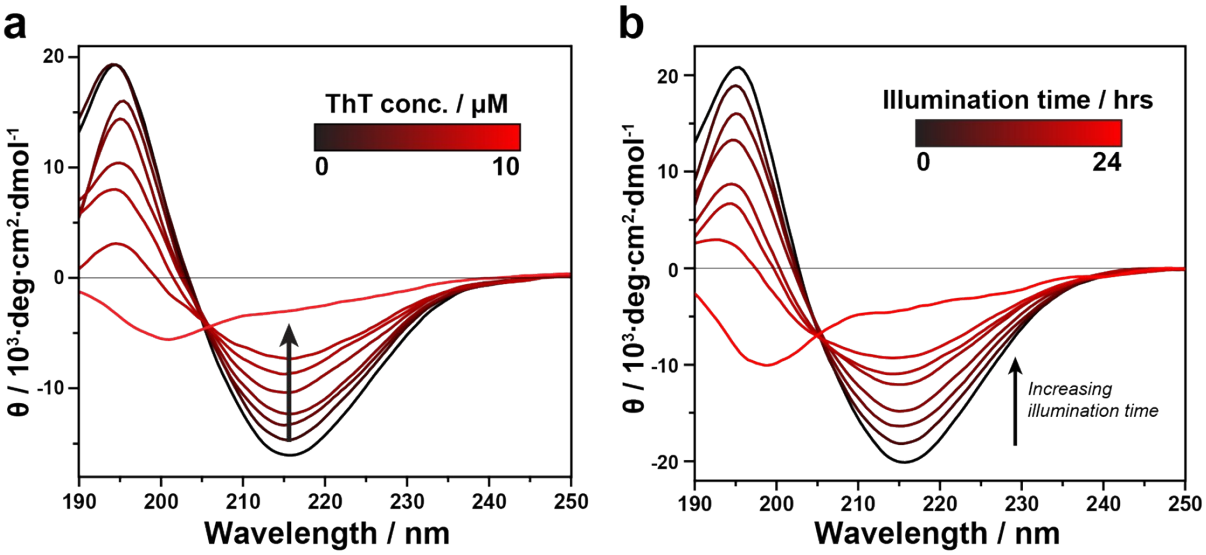

Figure S3. (a) CD spectra of $A\beta_{42}$ solutions treated with various concentrations (0, 0.1, 0.2, 0.5, 1, 2, and 10 μM) of ThT under light conditions. (b) The effect of different light exposure times (0, 0.5, 1, 2, 3.5, 6, 12, and 24 h) on the inhibitory activity of ThT.

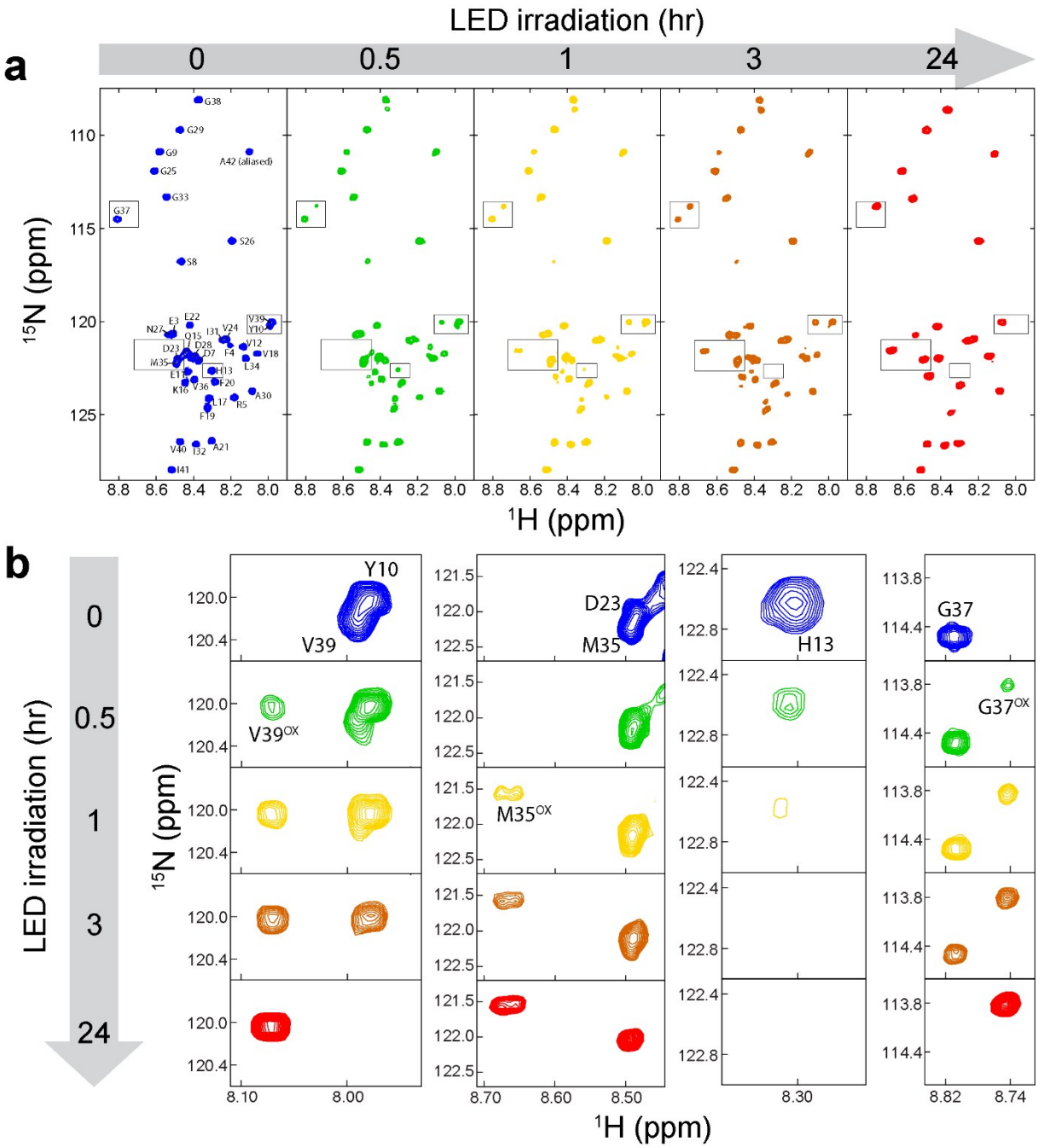

Figure S4. Time evolution of the ^{1}H-^{15}N HSQC spectra of Aβ$_{42}$ with ThT and LED irradiation. (a) Spectra of Aβ$_{42}$ (20 μM) with ThT (20 μM) were recorded for 20 min at 4 °C after each incubation time. (b) Time evolution of the key residues that show the signs of oxidation in the regions of HSQC spectra shown in (a). V39, M35 and G37 show both the decrease and increase in the intensities of the non-oxidized and oxidized peaks, respectively, indicating the oxidation of M35 as in the previous data.[6] Y10 and H13 also show reduction in the intensities of the non-oxidized peaks with increasing incubation time with LED light due to the oxidation of these residues that are further confirmed by mass spectrometry.

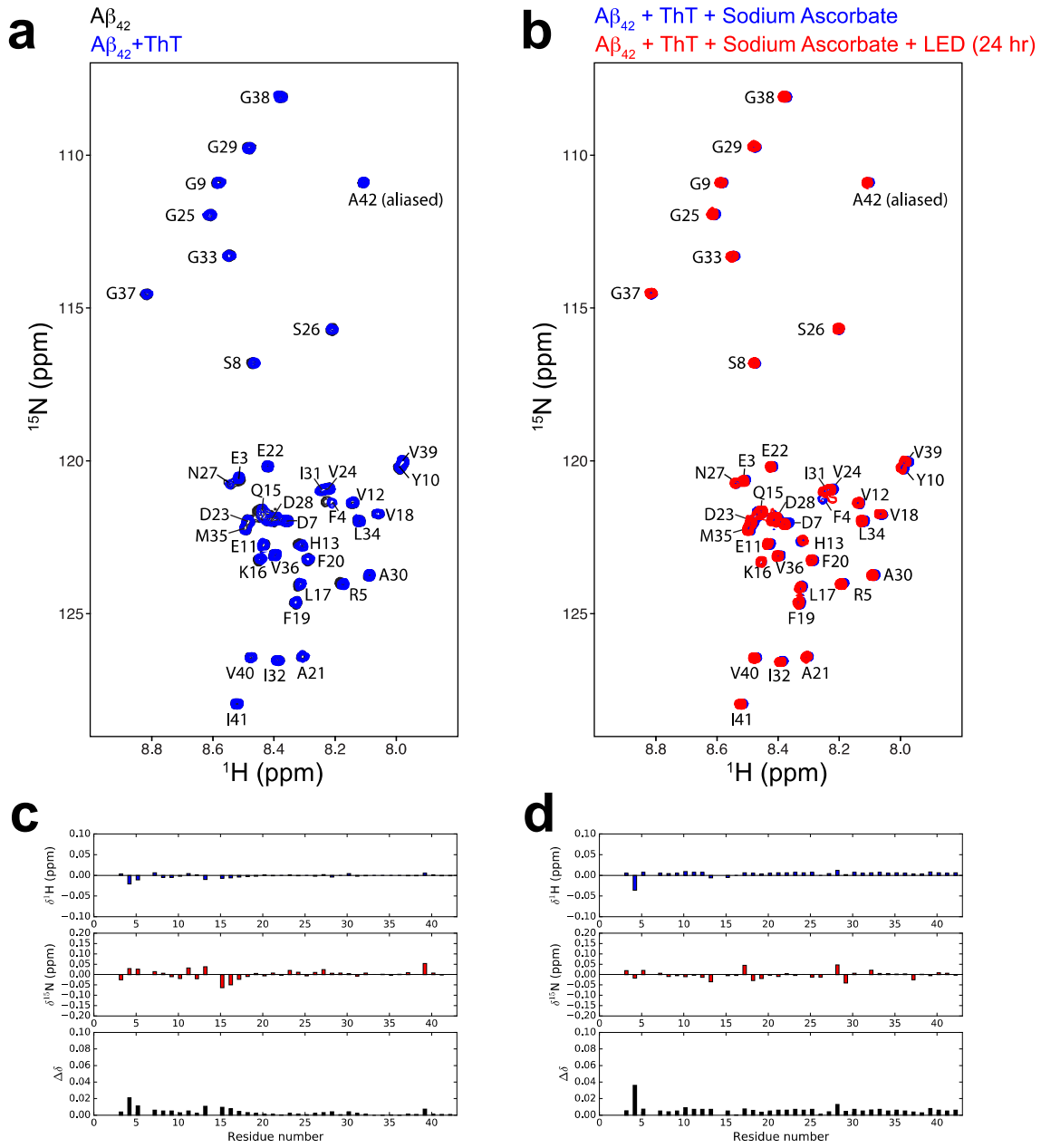

Figure S5. The effects of ThT and sodium ascorbate on Aβ$_{42}$ on ^{1}H-^{15}N HSQC spectra. (a) Spectrum of Aβ$_{42}$ (20 μM) before (black) and after (blue) addition of ThT (20 μM). All the amide cross-peaks have effectively unchanged identical chemical shifts, indicating no detectable signs of direct interaction between Aβ$_{42}$ and ThT molecules. (b) Aβ$_{42}$ (20 μM) before (blue) and after (red) incubation (20 hr) with ThT (20 μM) and LED irradiation in the presence of sodium ascorbate (1 mM). The amide resonances show effectively identical chemical shifts before and after incubation with sodium ascorbate, showing no signs of oxidation of Aβ$_{42}$. (c) - (d) Chemical shift perturbations from (a) and (b). δ^{1}H (top), δ^{15}N (middle) and the weighted difference ($\Delta\delta$, bottom) are shown against residue numbers. The value of the relative gyromagnetic ratios of ^{15}N and ^{1}H was used as the weighting factor ($\omega = \gamma_{15N}/\gamma_{1H}$) for calculating $\Delta\delta = ((\delta^{1}H)^2 + (\omega\delta^{15}N)^2)^{0.5}$.

Table S1. Trypsin proteolysis LC-MS/MS data from the fragments of $A\beta_{42}$ and oxidised $A\beta_{42}$. The expected and observed mass of each peptide fragment and the differences between these values are shown in Da and ppm, respectively. The predicted changes are obtained from the Mascot search (v2.3.02, Matrix Science) using Protein Discoverer.[8]

Residue	Sequence	$A\beta_{42}$			oxidized $A\beta_{42}$			Predicted change
		$M_{expected}$	$M_{observed}$	ppm	$M_{expected}$	$M_{observed}$	ppm	
0 – 5	MDAEFR	767.3272	767.3263	1.23	783.3221	783.3224	0.38	Oxidation (M0)
0 – 16	MDAEFRHDSGYEVHHQK	2084.9123	2084.9201	3.77				n/a
0 – 28	MDAEFRHDSGYEVHHQKL VFFAEDVGSNK				3471.5426	3471.5473	1.35	Oxidation (M0, Y10, H13, H14)
6 – 16	HDSGYEVHHQK	1335.5956	1335.5978	1.6				n/a
17 – 28	LVFFAEDVGSNK	1324.6663	1324.6703	2.98	1324.6663	1324.6714	3.81	n/a
29 – 42	GAIIGLMVGGVVIA				1284.7416	1284.7488	0.93	Oxidation (M35)

1

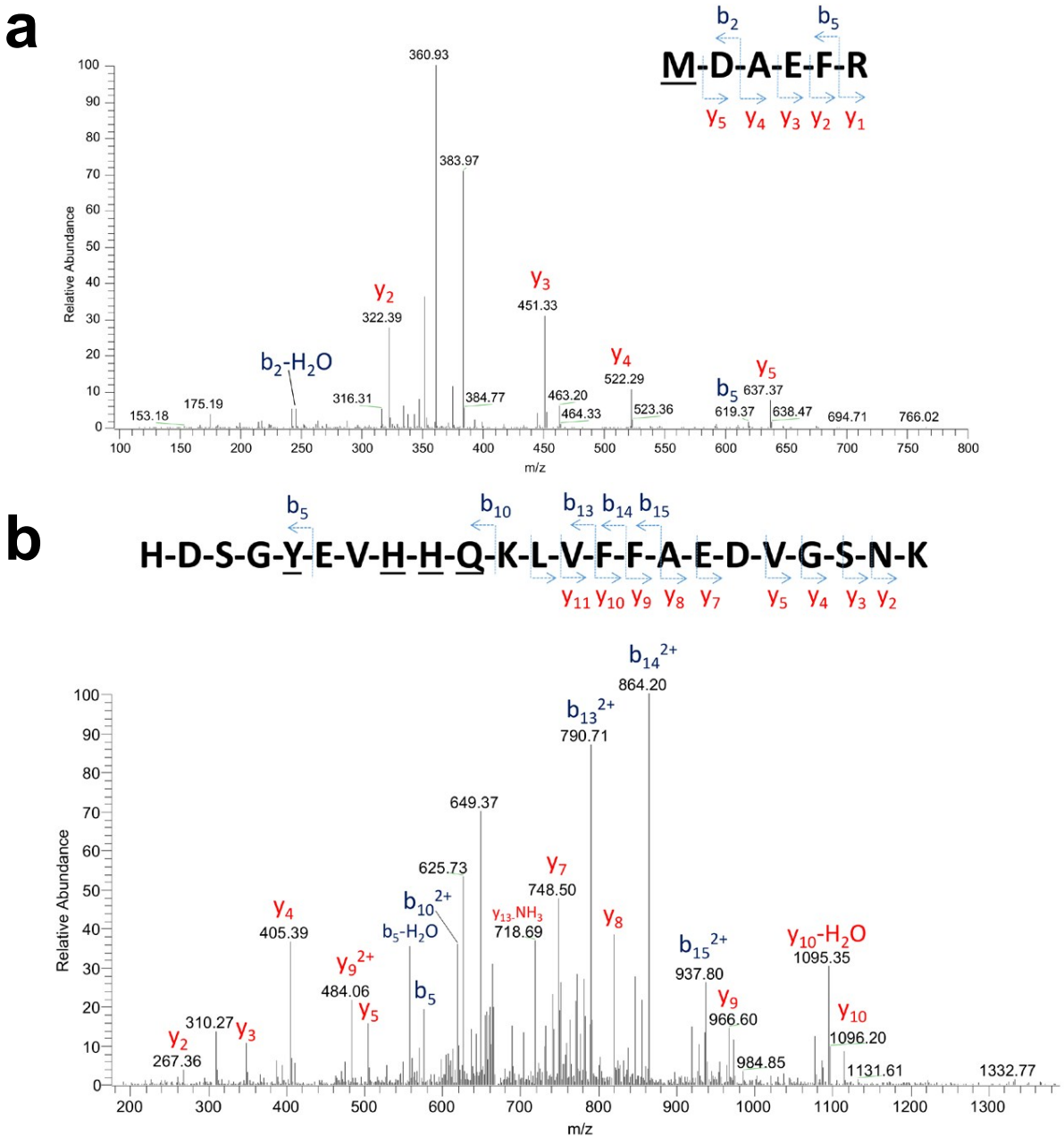
a
b2
b5
M-D-A-E-F-R
y5 y4 y3 y2 y1
Relative Abundance
m/z
360.93
383.97
y2
322.39
y3
451.33
b2-H2O
y4
522.29
y5
b5 637.37
316.31
384.77
463.20
464.33
523.36
619.37
638.47
694.71
766.02
153.18
175.19
b
b5
b10
b13 b14 b15
H-D-S-G-Y-E-V-H-H-Q-K-L-V-F-F-A-E-D-V-G-S-N-K
y11 y10 y9 y8 y7 y5 y4 y3 y2
b14 2+
864.20
b13 2+
790.71
649.37
625.73
y7
748.50
b10 2+
y13-NH3
718.69
y8
y4
405.39
b5-H2O
y9 2+
484.06
b5
y5
b15 2+
937.80
y10-H2O
1095.35
y9
966.60
y10
1096.20
310.27
y3
y2
267.36
984.85
1131.61
1332.77

2

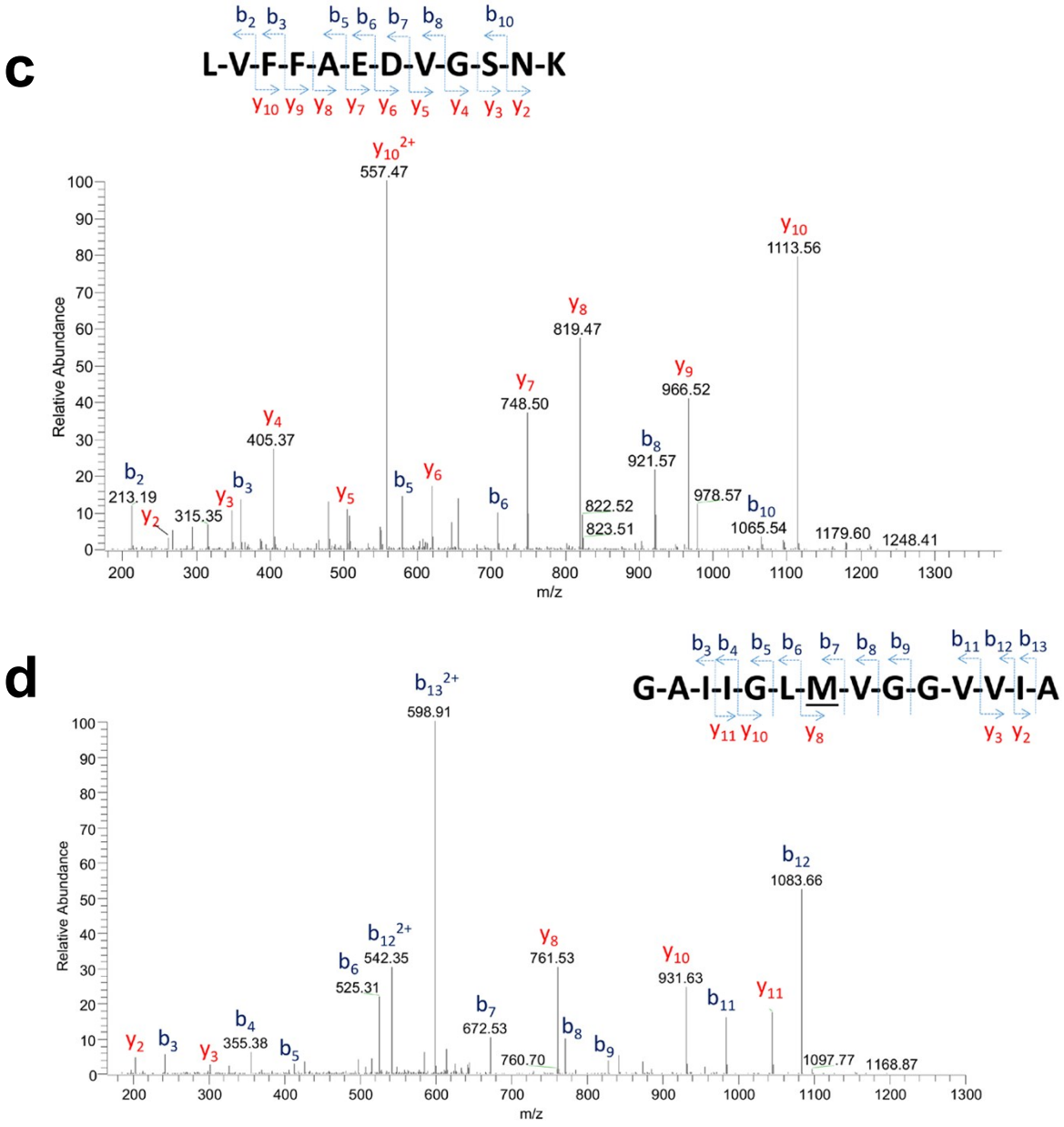

Figure S6. The MS/MS spectra of the fragments of oxidized Aβ$_{42}$ in Table S1. The peptide fragments are produced by trypsin digestion of oxidized Aβ$_{42}$ monomers. In the spectra, b-ions (blue) and y-ions (red), generated by the cleavage of peptide bonds are labeled.[9] Inset: amino acid sequence of each fragment with the detected b-ions and y-ions of the peptide fragments are indicated.

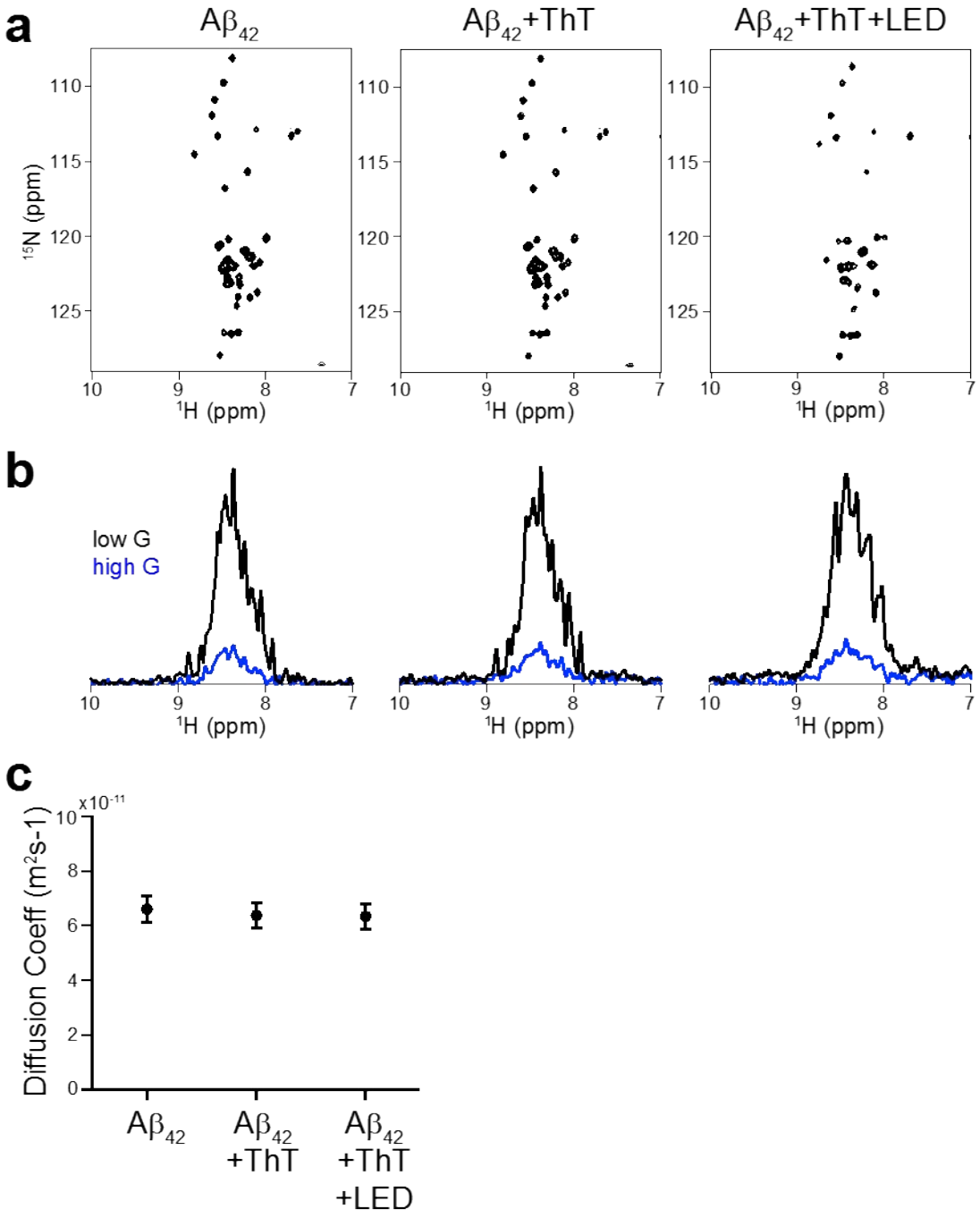

Figure S7. Translational diffusion measurements from NMR experiments. (a) SOFAST-HMQC ^{1}H-^{15}N spectra of $A\beta_{42}$ (50μM) in the absence (left) and presence (middle) of ThT (100μM) before and after (right) the incubation with LED irradiation for 20 hr at 4 °C. (b) ^{15}N SORDID spectra acquired at two different gradient strengths (G = 10.4 %, 69.5 % G_{max}).[3] (c) Diffusion coefficient calculated from (b) using Stejskal-Tanner equation,[7] $I/I_0 = \exp[-D\gamma^2\sigma^2G^2\delta^2(\Delta-\delta/3-\tau/2)]$, where D is diffusion coefficient, γ is the gyromagnetic ratio, δ is the length of the encoding and decoding gradient pulses (4 ms), σ is the shape factor of the gradient pulse (0.9 for the trapezoidal gradient shapes in this work), τ is the delay between the bipolar gradient pulses, and Δ is the diffusion delay (190 ms).

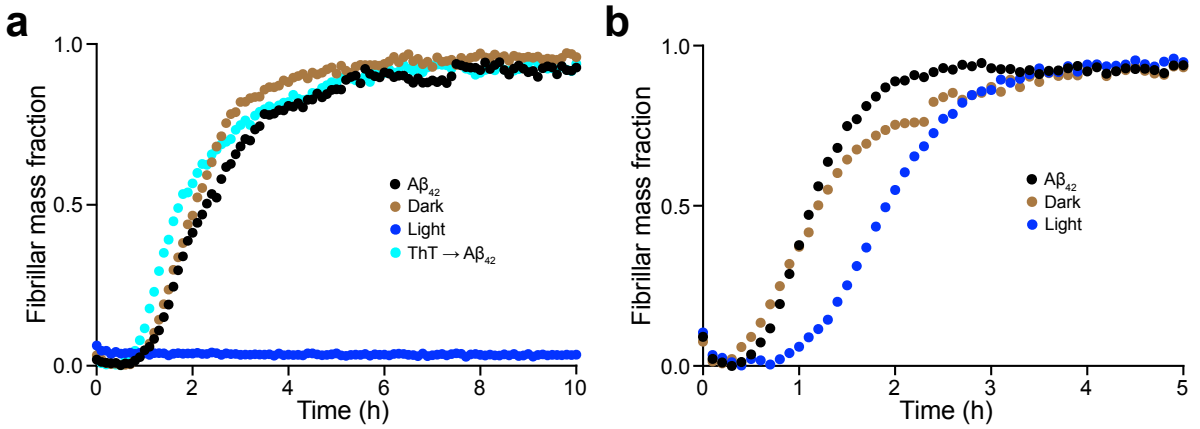

Figure S8. Aggregation kinetics of 2 μM $A\beta_{42}$ with ThT and LED light at 37 °C. (a) $A\beta_{42}$ pre-incubated in the absence (black) and presence of 2 μM ThT with (blue) and without (brown) light irradiation at 4 °C for 24 hr prior to the measurement of the aggregation kinetics. The sample containing 2 μM ThT for pre-incubation with LED light (cyan) to which fresh 2 μM $A\beta_{42}$ was added just before the start of aggregation kinetics showed no difference to the $A\beta_{42}$ only (black) or the dark sample. (b) The same experiments as in (a) but with 1 μM ThT.

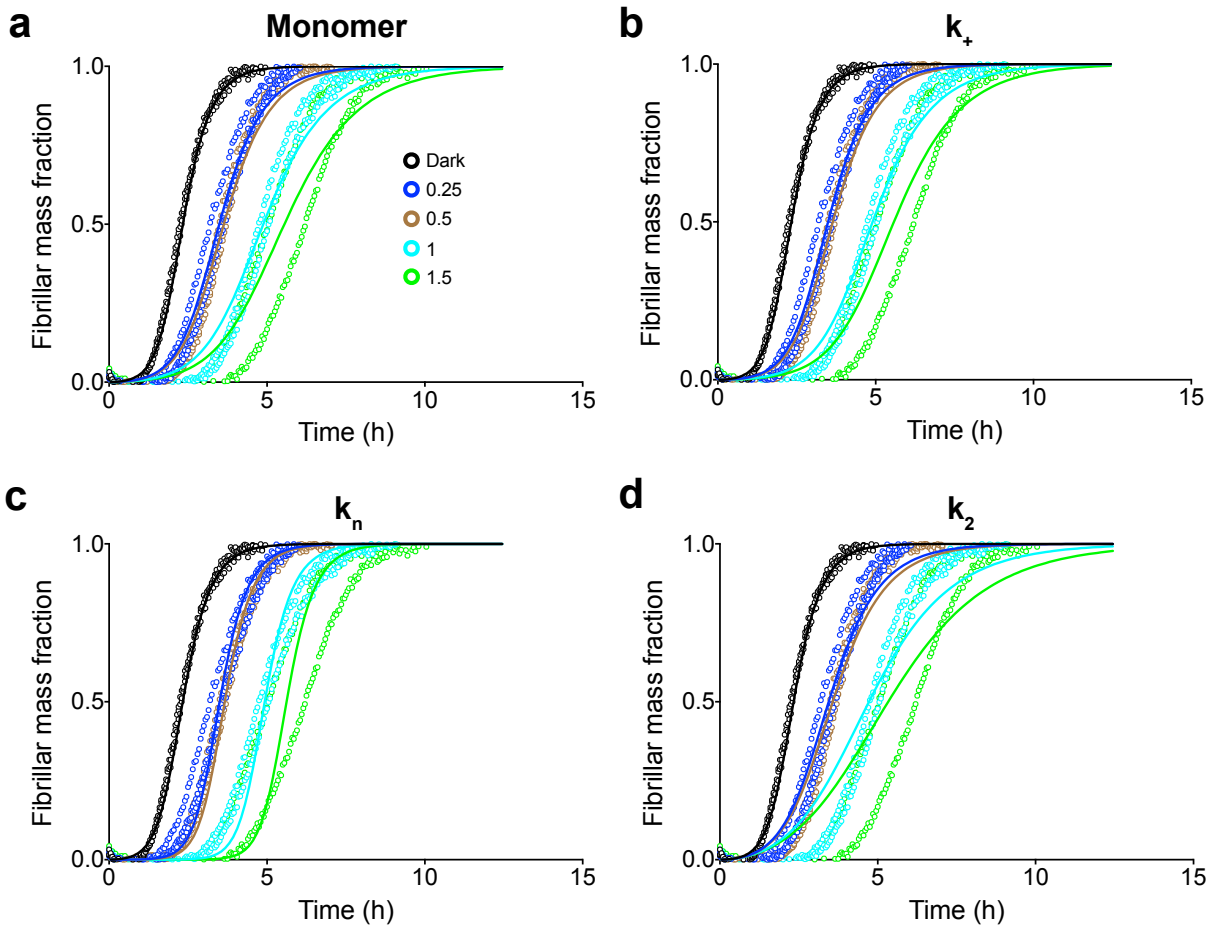

Figure S9. Normalized aggregation profiles from Figure 3(a) with fits from the kinetic analysis. Solid lines show predictions of the results using single fits, allowing inhibition only as a result of the changes in the monomer concentration (a), and elongation rate (b), and the primary (c) and secondary (d) nucleation, respectively.

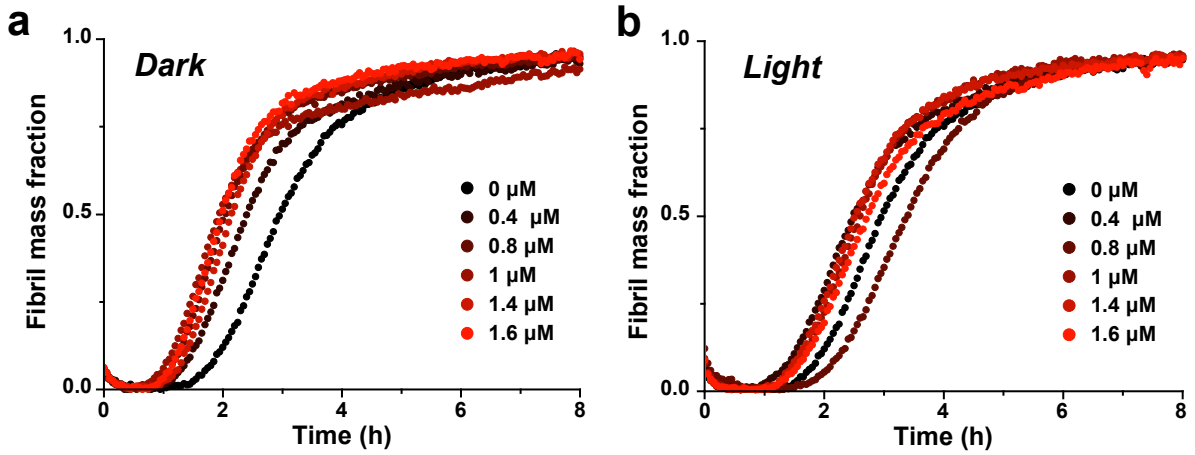

Figure S10. Normalized aggregation kinetics of 2 μM $A\beta_{42}$ with different concentrations of $A\beta_{42}$ pre-incubated with ThT in the absence (dark) and presence (light) of LED light irradiation shown in Figure 3(d) and (e). For the pre-incubation process, 2 μM $A\beta_{42}$ was used in the presence of 20 μM ThT under light and dark conditions at 4 °C for 24 hr. Different molar equivalents of these samples were added to 2 μM $A\beta_{42}$ prior to measurement of the aggregation kinetics.

References

[1] J. Habchi, S. Chia, R. Limbocker, B. Mannini, M. Ahn, M. Perni, O. Hansson, P. Arosio, J. R. Kumita, P. K. Challa, S. I. Cohen, S. Linse, C. M. Dobson, T. P. Knowles, M. Vendruscolo, *Proc. Natl. Acad. Sci. U. S. A.* **2017**, *114*, E200-E208.

[2] F. Delaglio, S. Grzesiek, G. W. Vuister, G. Zhu, J. Pfeifer, A. Bax, *J. Biomol. NMR* **1995**, *6*, 277-293.

[3] S. H. S. Chan, C. A. Waudby, A. M. E. Cassaignau, L. D. Cabrita, J. Christodoulou, *J. Biomol. NMR* **2015**, *63*, 151-163.

[4] E. Hellstrand, B. Boland, D. M. Walsh, S. Linse, *ACS Chem. Neurosci.* **2010**, *1*, 13-18.

[5] a) S. I. Cohen, M. Vendruscolo, C. M. Dobson, T. P. Knowles, *J. Mol. Biol.* **2012**, *421*, 160-171; b) S. I. A. Cohen, S. Linse, L. M. Luheshi, E. Hellstrand, D. A. White, L. Rajah, D. E. Otzen, M. Vendruscolo, C. M. Dobson, T. P. J. Knowles, *Proc. Natl. Acad. Sci. U. S. A.* **2013**, *110*, 9758-9763.

[6] a) L. Hou, H. Shao, Y. Zhang, H. Li, N. K. Menon, E. B. Neuhaus, J. M. Brewer, I.-J. L. Byeon, D. G. Ray, M. P. Vitek, T. Iwashita, R. A. Makula, A. B. Przybyla, M. G. Zagorski, *J. Am. Chem. Soc.* **2004**, *126*, 1992-2005; b) Y. Yan, S. A. McCallum, C. Wang, *J. Am. Chem. Soc.* **2008**, *130*, 5394-5395.

[7] E. O. Stejskal, J. E. Tanner, *The Journal of Chemical Physics* **1965**, *42*, 288-292.

[8] M. Brosch, L. Yu, T. Hubbard, J. Choudhary, *J. Proteome Res.* **2009**, *8*, 3176-3181.

[9] a) P. Roepstorff, J. Fohlman, *Biomed. Mass Spectrom.* **1984**, *11*, 601; b) C. Schöneich, T. D. Williams, *Chem. Res. Toxicol.* **2002**, *15*, 717-722.